IDENTIFYING COMPUTER GENERATED GRAPHICS VIA HISTOGRAM FEATURES

Ruoyu Wu, Xiaolong Li and Bin Yang

Institute of Computer Science and Technology, Peking University, Beijing 100871, China

ABSTRACT

Discriminating computer generated graphics from photographic images is a challenging problem of digital forensics. An important approach to this issue is to explore usual image statistics. In this way, when the statistical distributions (i.e., histograms) of some types of residual images are established, previous works usually apply operations on these histograms or compute statistical quantities to extract features. However, as the histograms are fundamental resources and can present most image information, the histograms themselves can be directly used as features and we do not need further manipulations on them. Based on this consideration, we simply take several highest histogram bins of the difference images as features to carry out classification, and these simple histogram features work well in terms of both detection accuracy and computational complexity. Actually, experimental results demonstrate that, with only 112 features, the proposed method outperforms some state-of-the-art works.

Index Terms— Digital forensics, computer generated graphics, photographic images

1. INTRODUCTION

Owing to the fast development in computer graphic technology, it is easier to use rendering software to generate graphics. Computer generated graphics (CGG) may be used in movie industry as fantastic scenes which are hard to present in real world, while they may be used for image forgery and even for criminal purpose. Nowadays, CGG are so photorealistic that people can hardly distinguish them from photographic images (PI). In this light, an automatic classification system is highly desired. Dealing with this issue serves two purposes. On one hand, it encourages computer graphics researchers to improve their algorithms to imitate the physical world more realistically. On the other hand, if the classification system is effective enough, it will serve as a powerful tool to reveal image forgery.

Numerous methods have been proposed to identify CGG and PI, and they can be roughly classified into two types:

- *Acquisition-process-based methods:* This type of methods is based on the differences in generation process of CGG and PI. Notice that for PI, the generation process includes many common processing stages whatever the digital camera is, and it leaves a unique signature in the resulting image which may not present in CGG, since CGG are produced by a graphics rendering pipeline which is a totally different process from PI. For instance, motivated by the physical CGG generation process, Ng *et al.* [1] introduced some geometry features to carry out classification; based on the modelisation of camera sensor pattern noise which is only presented in PI, Dehnie *et al.* [2] extracted features from the residual images derived by wavelet de-noising; Dirik *et al.* [3] explored the traces of demosaicking and chromatic aberration in PI to build features.
- *Statistical-distribution-based methods:* The basic idea of this type of methods is that, CGG and PI can be distinguished by utilizing some usual image statistics (such as those used in steganalysis), while the specific generation process of CGG and PI is considered as a "black-box" and not investigated. For instance, in wavelet domain, Lyu and Farid [4] utilized the first four order statistics of subband coefficients and inter-subband prediction-errors as features; also in wavelet domain, Wang and Moulin [5] extracted features from the characteristic functions of wavelet coefficient histograms; in [6], Chen *et al.* considered the moment-based features which are previously introduced in blind steganalysis. Besides, the methods [7] and [8] also belong to this type.

For either CGG or PI, the generation process is evidently complicated and very hard to describe by a universal model. Meanwhile, after generated, CGG and PI may undergo many uncontrollable and unpredictable manipulations such as usual signal processing operations, data embedding, etc. So the first approach is difficult to follow and recent works are mainly based on the second approach. Although the second approach does not model image generation process explicitly, it performs rather well according to the experimental results reported in [4–8]. We then focus on the second approach in this paper to construct more reliable statistical features for identifying CGG, and we show that some simple image statistics are capable of dealing with this classification problem.

In brief, we simply compute histograms of the difference images (i.e., the images composed of differences of adjacent pixels), then we take some highest (in other words, the most informative) histogram bins as features to represent image statistics to carry out classification. Noticing that these histograms are usually Laplacian-like distributions centered at the origin, the selected bins are located around 0. In this way, with only 112 features, the proposed method provides a superior performance to some state-of-the-art works which employ much more features.

The rest of this paper is organized as follows. Some related works are briefly introduced in Section 2. Then the proposed method is detailed in Section 3, followed by the experimental results reported in Section 4. Finally, the conclusions are drawn in the last section.

2. RELATED WORKS

The previous statistical-distribution-based methods [5–7] are briefly introduced and discussed in this section.

In [5], features are extracted from the characteristic functions of wavelet coefficient histograms. For each color component of RGB, the image is decomposed into three levels by Haar wavelet transform, and there are four subbands in each level: smooth, horizontal, vertical and diagonal. Besides, the first-level diagonal subband is further decomposed into four subbands. Accordingly, they have 48 subbands. For every subband, discrete Fourier transform (DFT) is performed on its histogram to obtain the characteristic function.

Corresponding author: Bin Yang, e-mail: yangbin@icst.pku.edu.cn

Fig. 1. Feature extraction mechanism of the previous statistical-distribution-based methods.

Then, three features are computed using the characteristic function: two features are inspired by the previous steganalytic method [9], which convey information about high-frequency components; and one new feature is devised to convey information about low- to mid-frequency components. Finally, a 144-D feature set is built.

In [6], the moments of characteristic functions of wavelet coefficient histograms are taken as features. Similar to [5], for each color component of HSV, the image is also decomposed into three levels based on Haar wavelet transform. So there are 13 subbands if the component image itself is considered as a subband at level 0. In addition, the prediction-error image derived by the median edge detector (i.e., MED) is taken into account, and the same decomposition is also applied to this image. A set of 78 subbands is obtained. Then for every subband, the characteristic function of its histogram is computed using DFT. Finally, the first three moments of each characteristic function are extracted, resulting in a 234-D feature set.

In the recent work [7], the image is changed to a JPEG 2-D array, which has the same size as the original image with each consecutive and non-overlapping 8×8 block filled up with the corresponding absolute values of quantized block DCT coefficients. Then the authors apply the Markov process to model this JPEG 2-D array and extract features from the transition probability matrix (TPM). More specifically, the 1-D and 2-D histograms of difference image of the JPEG 2-D array are first established, then the one-step TPM is computed using the two histograms, and finally, the elements of TPM are extracted as features. Taking the horizontal and vertical difference into account, and generating features from Y and Cb component together, this method has a 324-D feature set.

After the above presentation, we see that the basic feature extraction mechanism of the previous statistical-distribution-based methods can be summarized as follows (see Fig. 1). First, residual images which reflect image spatial correlations are obtained according to a certain transform. Then the statistical distributions (i.e., histograms) of residual images are established. Finally, after manipulating the histograms, the feature set is built by computing some certain quantities. For instance, reviewing Wang and Moulin's method [5], each subband of wavelet decomposition can be viewed as a residual image, and features are extracted after performing DFT on the histograms of residual images. In conclusion, the key point of these methods is clearly the utilization of histograms of residual images, and suitable image statistics may distinguish CGG from PI well.

3. THE PROPOSED METHOD

It is assumed and widely accepted that some statistical distributions of CGG and PI are distinguishable. This observation provides an approach to identify CGG, where the main problem is to select and describe statistical distributions correctly. To deal with this issue, when the histograms are established, previous methods usually apply operations (e.g., DFT [5, 6]) on these histograms or compute statistical quantities (e.g., mean, variation, skewness and kurtosis [4]) to extract features. However, notice that the histograms are fundamental resources and can present most image information, we argue that the histograms themselves can be directly used as features and actually we do not need further manipulations on them. Our idea is detailed as follows.

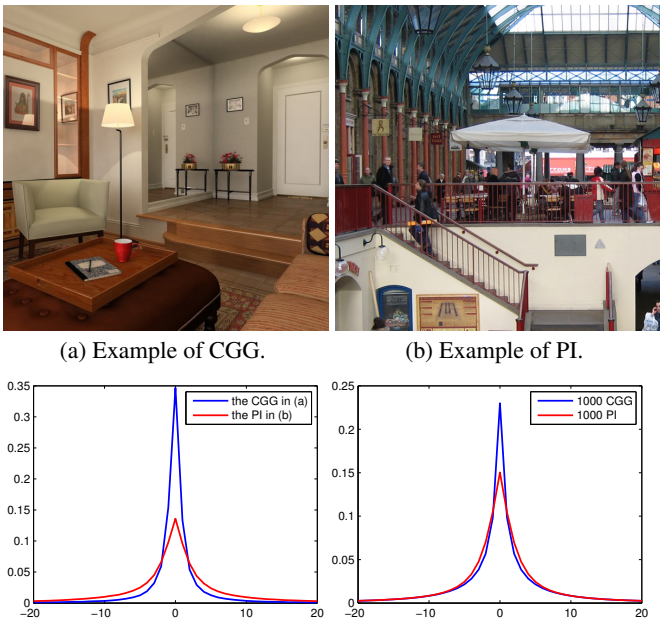

(a) Example of CGG. (b) Example of PI.

(c) Difference-histograms of (a) and (b). (d) Average difference-histograms of 1000 CGG and 1000 PI.

Fig. 2. Examples of CGG and PI, and comparisons of histograms of difference images. Here, the difference images are computed in R component of RGB.

We consider the simplest residual image: the difference image in horizontal direction. Here we remark that the difference image has already been widely adopted in steganalysis [10, 11]. For a given image I, its horizontal difference image is defined as $I_h = I * f_h$, where f_h is the horizontal convolution kernel $(1, -1)$. Then we compute the normalized histogram H_h:

$$H_h(n) = \frac{\sharp\{(i,j) : I_h(i,j) = n\}}{N}, \qquad -255 \le n \le 255,$$

where N is the total number of pixels in I_h, and $\sharp$ denotes the cardinal number of a set. Let us see Fig. 2. Examples of CGG and PI are presented in Fig. 2(a) and 2(b), and comparison of histograms of their difference images is shown in Fig. 2(c). According to this comparison, we observe that the difference-histogram of CGG has a much higher peak point with more rapid two-sided decay. Thus, for this example, the difference-histogram has good discrimination. Actually, this practical observation is a general phenomenon. Referring to Fig. 2(d), it shows the averages of difference-histograms for 1000 CGG and 1000 PI, and we observe the same discrimination.

Some primary experimental results are presented here. Fig. 3(a) shows the peak point $H_h(0)$ of difference-histogram, for 1000 CGG (blue points) and 1000 PI (red points). Obviously, the peak point is relatively large for CGG and thus this quantity is profitable if using it for CGG detection. In Fig. 3(b), the point $(H_h(0), H_h(1))$ is plotted, also for 1000 CGG (blue points) and 1000 PI (red points). From this figure, we see that in contrast to blue points, the red ones are more compactly distributed. We then use $\{H_h(0), ..., H_h(k)\}$ which contains $1+k$ elements as a feature set to detect CGG, where $k \ge 0$ is a preselected integer. The corresponding receiver operating characteristic (ROC) curves are shown in Fig. 3(c). Clearly, we can detect CGG to some extent with only one feature though the performance is not favorable, and the detection rate increases if employing

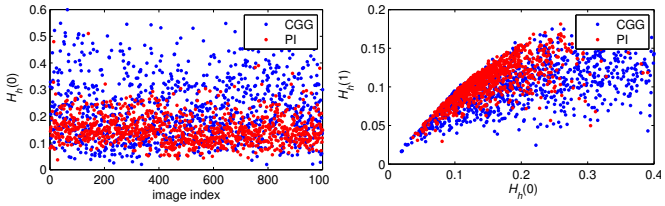

(a) Peak point of difference-histogram, for 1000 CGG and 1000 PI.

(b) Point $(H_h(0), H_h(1))$, for 1000 CGG and 1000 PI.

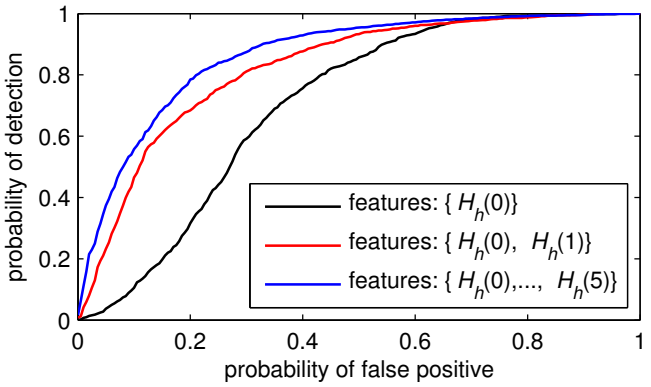

(c) ROC curves of CGG detection using different features.

Fig. 3. Illustration of the effectiveness of histogram features.

more features. Moreover, the detection performance is rather good with just six features, for instance, we can get a detection rate about 80% when the probability of false positive (percentage of PI that are misclassified as CGG) is 20%. These experiments illustrate well that these simple histogram features are valuable in CGG detection.

We now give the feature extraction procedure of the proposed method (see Fig. 4 for an illustration). Notice that the horizontal difference image only reflects the first-order image statistics in one direction. We may simultaneously utilize difference images in other directions and second-order statistics (i.e., the difference images of difference images). In addition, as the difference-histogram is symmetric to 0, we simply take the following features in order to reduce the feature dimension:

$$H(0), \frac{H(1)+H(-1)}{2}, ..., \frac{H(k)+H(-k)}{2}, \qquad (1)$$

where H is a given difference-histogram.

Taking into account these considerations, we extract features as follows. First, compute the first-order and second-order difference images: $I_i = I * f_i$ and $I_{i,j} = I * f_i * f_j$, where $i, j \in \{h, v, d, a\}$ and f_i are convolution kernels in four directions (horizontal, vertical, diagonal, anti-diagonal):

$$f_h = (1, -1), f_v = \begin{pmatrix} 1 \\ -1 \end{pmatrix}, f_d = \begin{pmatrix} 1 & 0 \\ 0 & -1 \end{pmatrix}, f_a = \begin{pmatrix} 0 & 1 \\ -1 & 0 \end{pmatrix}.$$

Notice that $I_{i,j} = I_{j,i}$ holds for each $i, j \in \{h, v, d, a\}$, and we get 14 difference images in total. Then, for each difference image, compute its histogram H and take $1 + k$ features according to Eq. (1). Thus we get a feature set containing $14(1+k)$ features. Finally, we use these features to train and test.

The experimental results including performance evaluation of our method and comparisons with state-of-the-art works will be reported in the next section.

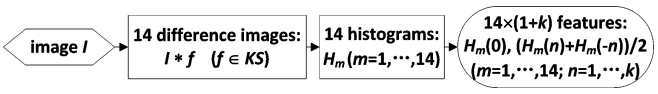

Fig. 4. Feature extraction procedure of the proposed method, where KS is a kernel set which contains 14 kernels.

Table 1. Performance of the proposed method measured by detection accuracy and AUC, for different parameter k.

	accuracy			AUC		
k	R	G	B	R	G	B
0	79.9%	78.8%	81.8%	0.887	0.878	0.891
1	88.8%	89.0%	87.9%	0.944	0.943	0.935
2	92.6%	92.8%	91.8%	0.970	0.974	0.960
3	94.3%	94.0%	94.4%	0.982	0.982	0.985
4	94.3%	94.1%	95.0%	0.984	0.983	0.987
5	94.8%	94.5%	95.0%	0.985	0.985	0.987
6	94.9%	94.7%	95.2%	0.985	0.986	0.989
7	95.2%	95.1%	95.3%	0.987	0.988	0.988
8	95.0%	95.1%	95.4%	0.986	0.988	0.990
9	94.9%	95.0%	95.4%	0.986	0.988	0.990
10	95.1%	94.9%	95.2%	0.987	0.987	0.989
11	95.0%	95.0%	95.1%	0.986	0.987	0.988
12	95.0%	94.9%	95.1%	0.985	0.987	0.988
13	94.8%	95.0%	95.2%	0.984	0.987	0.987
14	94.7%	94.9%	95.0%	0.985	0.987	0.988
15	94.7%	95.0%	94.8%	0.985	0.988	0.987
16	94.5%	94.8%	95.1%	0.984	0.987	0.987
17	94.6%	94.9%	94.8%	0.984	0.988	0.986
18	94.5%	94.5%	94.8%	0.985	0.987	0.986
19	94.0%	94.6%	94.8%	0.982	0.987	0.986
20	94.5%	94.3%	94.6%	0.983	0.986	0.986

4. EXPERIMENTAL RESULTS

All the CGG and PI in our database are RGB color images downloaded from various internet websites. The CGG database contains 1000 images sized from 400×400 to 1600×1600 with moderate to good visual quality. The PI database contains 1000 digital camera images sized 1024×1024 with very good visual quality. These images are collected from more than 50 types of digital cameras where the original images are in RAW or lossless JPEG format with size from 2000×2000 to 4000×4000, and we crop a 1024×1024-sized block in each selected image to form the PI database. The images in our database consist of a variety of outdoor and indoor scenes, including nature (e.g., flowers, trees, animals), portraits, man-made objects (e.g., architectures), etc.

The proposed method is tested in each R, G and B component, and we use the parameter-independent classifier FLD (Fisher linear discriminant) to train and test. In each experiment, we choose 80% of CGG and 80% of PI for training, and the remaining 20% for testing. The procedure is repeated 10 times for 5-fold cross-validation and the ROC curves are vertically averaged. Our method is then evaluated by computing the detection accuracy and the area under ROC curve (AUC), and an accuracy/AUC close to 100%/1.0 indicates excellent discrimination. Tab. 1 shows the detection results for different parameter k. According to this table, the performance becomes better when k increases, while for $k \geq 7$, it changes a little and tends to the same. That is to say, our method can provide the best result with 112 features, balancing detection performance and

Table 2. Comparisons between the proposed method and previous works [5–7].

	feature size	TP	TN	accuracy
[5]	144	92.9%	89.1%	91.0%
[6]	234	94.6%	94.6%	94.6%
[7]	324	93.7%	91.3%	92.5%
proposed (R)	56 ($k = 3$)	94.9%	93.6%	94.3%
proposed (G)	56 ($k = 3$)	94.4%	93.6%	94.0%
proposed (B)	56 ($k = 3$)	94.5%	94.3%	94.4%
proposed (R)	112 ($k = 7$)	95.7%	94.7%	95.2%
proposed (G)	112 ($k = 7$)	95.5%	94.6%	95.1%
proposed (B)	112 ($k = 7$)	95.7%	94.9%	95.3%

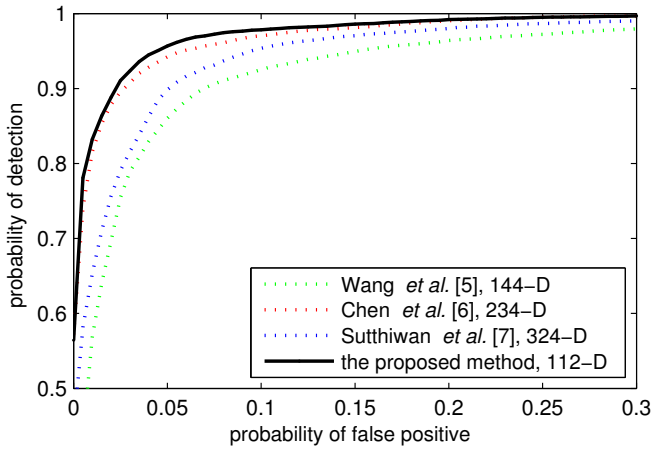

Fig. 5. Comparisons of ROC curves of CGG detection between the proposed method and previous works [5–7].

feature dimension. In addition, for fixed k, we can get very similar classification result for each R, G and B component.

The comparisons between our method and previous works [5–7] are presented as below. Here, we implement these algorithms ourselves, then we train and test according to the classifier and parameters mentioned in their papers on our image database:

- For [5], FLD is applied as classifier.
- For [6] and [7], support vector machine (SVM) is applied as classifier with radial basis function (RBF) kernel. Moreover, grid-search is used to find optimal penalty parameter and kernel parameter.

The train and test procedure for these algorithms is also repeated 10 times for 5-fold cross-validation. The comparison results are shown in Tab. 2, where TP (true positive) and TN (true negative) represent respectively the detection rate of CGG and PI, and the accuracy is actually the average of TP and TN. From this table, we see that our method with 112 features outperforms these state-of-the-art works with higher TP, TN and accuracy. Moreover, with only 56 features, our method performs similarly to [5–7] which employ much more features. In addition, we present the comparisons of ROC curves in Fig. 5. We see that the proposed method is slightly better than [6], while our improvement over [5] and [7] is significant.

Finally, we remark that the computational complexity of the proposed method is rather low since the transformations such as wavelet decomposition or DFT are not involved in feature extraction.

5. CONCLUSIONS

A novel method to identify CGG has been presented in this work, where the features used for classification are simply the histogram bins of first-order and second-order difference images. Compared to state-of-the-arts works, the proposed method is superior with higher detection accuracy, smaller feature dimension and lower computational complexity.

The tails of histograms, which are not considered in this paper, might be helpful for CGG detection. This point will be investigated in future. Besides, following the feature fusion idea of Sankar *et al.* [12], one of our works in progress is to combine different types of features to further improve the detection performance. Moreover, trying different color models and applying boosting-feature-selection are also valuable experimental tasks.

6. REFERENCES

[1] T.-T. Ng, S.-F. Chang, J. Hsu, L. Xie, and M.-P. Tsui, "Physics-motivated features for distinguishing photographic images and computer graphics," in *Proc. ACM Multimedia*, 2005, pp. 239–248.

[2] S. Dehnie, T. Sencar, and N. Memon, "Digital image forensics for identifying computer generated and digital camera images," in *Proc. IEEE ICIP*, 2006, pp. 2313–2316.

[3] A. E. Dirik, S. Bayram, H. T. Sencar, and N. Memon, "New features to identify computer generated images," in *Proc. IEEE ICIP*, 2007, vol. IV, pp. 433–436.

[4] S. Lyu and H. Farid, "How realistic is photorealistic," *IEEE Trans. Signal Process.*, vol. 53, no. 2, pp. 845–850, Feb. 2005.

[5] Y. Wang and P. Moulin, "On discrimination between photorealistic and photographic images," in *Proc. IEEE ICASSP*, 2006, vol. II, pp. 161–164.

[6] W. Chen, Y. Q. Shi, and G. Xuan, "Identifying computer graphics using HSV color model and statistical moments of characteristic functions," in *Proc. IEEE ICME*, 2007, pp. 1123–1126.

[7] P. Sutthiwan, X. Cai, Y. Q. Shi, and H. Zhang, "Computer graphics classification based on Markov process model and boosting feature selection technique," in *Proc. IEEE ICIP*, 2009, pp. 2913–2916.

[8] D. Chen, J. Li, S. Wang, and S. Li, "Identifying computer generated and digital camera images using fractional lower order moments," in *Proc. ICIEA*, 2009, pp. 230–235.

[9] G. Xuan, Y. Q. Shi, J. Gao, D. Zou, C. Yang, Z. Zhang, P. Chai, C. Chen, and W. Chen, "Steganalysis based on multiple features formed by statistical moments of wavelet characteristic functions," in *Proc. of the 7th International Workshop on Information Hiding*, 2005, vol. 3727 of *LNCS*, pp. 262–277.

[10] X. Li, T. Zeng, and B. Yang, "Detecting LSB matching by applying calibration technique for difference image," in *Proc. of the 10th ACM Workshop on Multimedia & Security*, 2008, pp. 133–138.

[11] Y. Sun, F. Liu, B. Liu, and P. Wang, "Steganalysis based on difference image," in *Proc. IWDW*, 2008, vol. 5450 of *Springer LNCS*, pp. 184–198.

[12] G. Sankar, V. Zhao, and Y.-H. Yang, "Feature based classification of computer graphics and real images," in *Proc. IEEE ICASSP*, 2009, pp. 1513–1516.